JBC RESEARCH ARTICLE

Palmitoylation of CYSTM (CYSPD) proteins in yeast

Received for publication, June 22, 2023, and in revised form, December 11, 2023 Published, Papers in Press, December 28, 2023,
https://doi.org/10.1016/j.jbc.2023.105609

María Luz Giolito[‡], **Gonzalo Bigliani**[‡], **Rocío Meinero**, **and Javier Valdez Taubas**[*]

From the Centro de Investigaciones en Química Biológica de Córdoba (CIQUIBIC), CONICET, and Departamento de Química Biológica Ranwel Caputto, Facultad de Ciencias Químicas, Universidad Nacional de Córdoba, Córdoba, Argentina

Reviewed by members of the JBC Editorial Board. Edited by Henrik Dohlman

A superfamily of proteins called cysteine transmembrane is widely distributed across eukaryotes. These small proteins are characterized by the presence of a conserved motif at the C-terminal region, rich in cysteines, that has been annotated as a transmembrane domain. Orthologs of these proteins have been involved in resistance to pathogens and metal detoxification. The yeast members of the family are YBR016W, YDL012C, YDR034W-B, and YDR210W. Here, we begin the characterization of these proteins at the molecular level and show that Ybr016w, Ydr034w-b, and Ydr210w are palmitoylated proteins. Protein S-acylation or palmitoylation, is a posttranslational modification that consists of the addition of long-chain fatty acids to cysteine residues. We provide evidence that Ybr016w, Ydr210w, and Ydr034w-b are localized to the plasma membrane and exhibit varying degrees of polarity toward the daughter cell, which is dependent on endocytosis and recycling. We suggest the names CPP1, CPP2, and CPP3 (C terminally palmitoylated protein) for YBR016W, YDR210W, and YDR034W-B, respectively. We show that palmitoylation is responsible for the binding of these proteins to the membrane indicating that the cysteine transmembrane on these proteins is not a transmembrane domain. We propose renaming the C-terminal cysteine-rich domain as cysteine-rich palmitoylated domain. Loss of the palmitoyltransferase Erf2 leads to partial degradation of Ybr016w (Cpp1), whereas in the absence of the palmitoyltransferase Akr1, members of this family are completely degraded. For Cpp1, we show that this degradation occurs *via* the proteasome in an Rsp5-dependent manner, but is not exclusively due to a lack of Cpp1 palmitoylation.

A superfamily of proteins called cysteine-rich transmembrane (CYSTM) proteins was identified using a bioinformatics approach (1). Members of this family were found to be widely distributed across eukaryotes (1). These proteins are in general small, ranging from 60 to 150 amino acids. The family was named CYSTM domain because they share a region at their C termini that was predicted to be an α-helical transmembrane region, containing 5 to 6 cysteine residues, which are highly conserved within the family. The N-terminal region is rich in proline, glycine, and glutamic acid and it is predicted to contain a β-strand region followed by a variable linker (1). In the yeast *Saccharomyces cerevisiae*, the family comprises the genes YBR016W, its paralog YDL012C, YDR034W-B, and YDR210W, with no defined function (1). The manganese-chelating protein (Mnc1) (YBR056W-A) has also been proposed to be a member of the CYSTM family (2). Mnc1 is a paralog of YDR034W-B, but does not have a CYSTM region as defined by Venancio *et al* (1), since it is not predicted to fold into a single α-helix (our unpublished observations). A role in manganese metabolism has also been proposed for Ydr034w-based both on a growth phenotype and its enhanced expression in the presence of this metal (3).

High-throughput studies indicate that the yeast members of this family are localized to the plasma membrane (PM) (4, 5). CYSTM-containing orthologs (1) include the *Schizosaccharomyces pombe* stress and chemical response protein Uvi15 (6), *Digitaria ciliaris*, and *Oryza sativa* CDT1, which confers resistance to heavy metals such as cadmium and copper (7) and the Arabidopsis representative of the family PCC1, which is induced upon pathogen exposure and its overexpression conferred resistance to oomycetes (8).

More recently, 13 CYSTM genes were identified in *Arabidopsis thaliana* (9). The expression of these genes was analyzed in different plant tissues and also in response to diverse stressors, leading to the postulate that they might have diverse roles in abiotic stress. Dimerization of some of these proteins was also suggested, based on two-hybrid experiments. Finally, they were shown to localize to the PM but also the cytosol and nucleus (9). A role in resistance to heat stress and to a lesser extent to UV radiation has been uncovered for two members of this family, also in *Arabidopsis* (10).

Expression of the human CYSTM1 gene is an early marker for Huntington's disease (11).

The genes YDL012C and YDR210W clustered in bioinformatics analyses based on the phenotypes of their corresponding deletion mutants, in the presence of a great variety of chemical compounds, suggesting they might be involved in resistance to stresses (1).

However, there is no data regarding the function of these proteins at the molecular level.

S-acylation, commonly known as palmitoylation, is the addition of long-chain fatty acid molecules to cysteine residues of a protein *via* a thioester bond. This modification is catalyzed by a family of palmitoyltransferases (PATs) characterized by

[‡] These authors contributed equally to this work.
[*] For correspondence: Javier Valdez Taubas, Javier.valdez@unc.edu.ar.
Present address for Gonzalo Bigliani: Centre for Genomic Regulation (CRG), The Barcelona Institute for Science and Technology, Barcelona, Spain.

the presence of a DHHC-CRD domain (12). Yeast has seven members of this family on its genome, and there are 23 members of this family in humans (12). Both transmembrane and peripheral membrane proteins can be modified by palmitoylation. The modification of otherwise soluble proteins results in their recruitment to membranes, often in combination with other signals such as prenylation, N-myristoylation, or a polybasic domain. Proteins can be anchored to membranes also by multiple palmitoylations, as is the case for the SNARE SNAP25 (reviewed in (13)). There are no consensus aminoacid sequences that dictate protein palmitoylation, and although the specificity of PATs in general, is incompletely understood, yeast PATs appear to have a preference for certain substrates. For instance, Erf2/Erf4 seem to modify heterolipidated proteins, Akr1 modifies hydrophilic proteins that bind to membranes through their palmitate moieties, Pfa4 modifies multispanning membrane proteins like amino acid permeases, while Swf1 recognizes single-spanning membrane proteins with cysteines close to the cytosolic border of their transmembrane domains (TMDs) (14, 15).

In this work, we have begun the characterization of three members of the yeast CYSTM family. We show that they are localized to the PM and polarized to the daughter cell, in a manner dependent on their endocytosis and recycling.

We provide abundant evidence that Ybr016w, Ydr210w, and Ydr034w-b are not transmembrane proteins, but are anchored to the membrane through S-acylation instead, and therefore suggest that the CYSTM is renamed to CYSPD (cysteine-rich palmitoylated domain [CYSPD]).

In light of these results, we suggest the names CPP1, CPP2, and CPP3 (cysteine-rich palmitoylated protein) for the genes YBR016W, YDR210W, and YDR034W-B, respectively.

Results

CYTSM proteins are polarized and palmitoylated

Based on the sequence of CYSTM domains, we suspected they might be modified by palmitoylation (Fig. 1*A*). There are several examples in the literature of cysteine-rich domains that are palmitoylated (reviewed in (16). Moreover, Ybr016w (CPP1) was identified as palmitoylated in the yeast palmitoylproteome (14).

To detect CYSTM proteins, we generated GFP fusions to the N termini of Ybr016w (Cpp1), Ydr210w (Cpp2), and Ydr034w-b (Cpp3) and expressed them from a centromeric plasmid, under the control of the constitutive TPI1 promoter. The resulting chimaeras were observed under the microscope. All three fusions are localized to the PM in a WT strain (Fig. 1*B* upper panels). GFP-Cpp1 showed a polarized distribution to the growing bud. Some proteins achieve a polarized distribution through cycles of endocytosis and polarized secretion. This was shown for the SNARE protein Snc1 (17). When Snc1 endocytosis was blocked, polarized distribution was lost, and the protein was homogeneously distributed in the PM. When recycling to the PM was blocked, the protein is trapped inside the cell (17). GFP-Cpp1 was expressed in *sla1Δ* mutant in which endocytosis is greatly reduced (18), and we can observe that the protein is no longer polarized (Fig. 1*B* middle panel). Ric1 is required for efficient fusion of endosome-derived vesicles with the Golgi, leading to impaired recycling of proteins from the endocytic compartments to the PM when it is absent (19). When we expressed GFP-Cpp1 in a *ric1Δ* strain, the protein is now found in internal structures (Fig. 1*B* bottom panel), indicating that GFP-Cpp1 is dynamically polarized through endocytosis and polarized secretion. An endocytosis signal on the N-terminal domain of Ybr016w was previously suggested (17).

GFP-Cpp2 and GFP-Cpp3 are also polarized on the PM but to a lesser extent. This polarity is lost in a *sla1Δ* strain and internal staining was observed for both proteins in a *ric1Δ* strain, although a substantial amount of the proteins remains at the PM (Fig. 1*B*, bottom panels), consistently with the partial polarization observed for these proteins in a WT strain.

To establish if the yeast CYSTM proteins are palmitoylated, we carried out acyl-biotin exchange (ABE) assays (14). Briefly, free thiols from cysteine residues in the protein samples are blocked by neutral N-ethylmaleimide and then treated with hydroxylamine (HA) to release thioester-bound palmitates. The free thiols are now reacted with a biotinylating agent, proteins are affinity-purified with streptavidin beads and the samples are analyzed for the presence of the GFP fusion proteins. Tris is used instead of HA as a control. Figure 1*C* shows that GFP-Cpp1, GFP-Cpp2, and GFP-Cpp3 are specifically pulled down in the HA-treated samples, indicating that they are palmitoylated.

Direct evidence for CYSTM proteins palmitoylation was obtained by metabolic labeling the cells with azido-palmitate, which can be later biotinylated using a click-chemistry approach. Palmitoylated proteins are then pulled down and identified by Western blot (20, 21). Figure 1*D* shows that GFP-Cpp1 and GFP-Cpp2 are present in the samples labeled with azido-palmitate (azido-palm) (top panel). The palmitoylated protein Vac8 (22) was detected, as a positive control (middle panel), while the non-palmitoylated Tom40 was used as a negative control. Since GFP-Cpp3 is expressed at lower levels than Cpp1 and Cpp2, we were unable to detect it using this technique.

Cpp1, Cpp2, and Cpp3 are bound to membranes via *palmitoylation*

If CYSTM domains are transmembrane domains as postulated, some of their cysteines would be close to the cytosolic border of the TMD (Cys 110 and Cys 114 for Cpp1, see Fig. 1*A*) and therefore candidates for palmitoylation (23–25). In yeast, cysteines on the cytosolic border of the TMDs are almost exclusively modified by Swf1 (14, 25). However, we and others have been unsuccessful in finding CYSTM proteins as substrates of Swf1. Moreover, a direct interaction between the PAT Akr1 and Cpp3 has been demonstrated in a protein-fragment complementation analysis (26). Additionally, transmembrane prediction algorithms do not consistently indicate that the CYSTMs are TMDs. Running Cpp1 on the TopoloGYeast website (27), which provides the predictions from

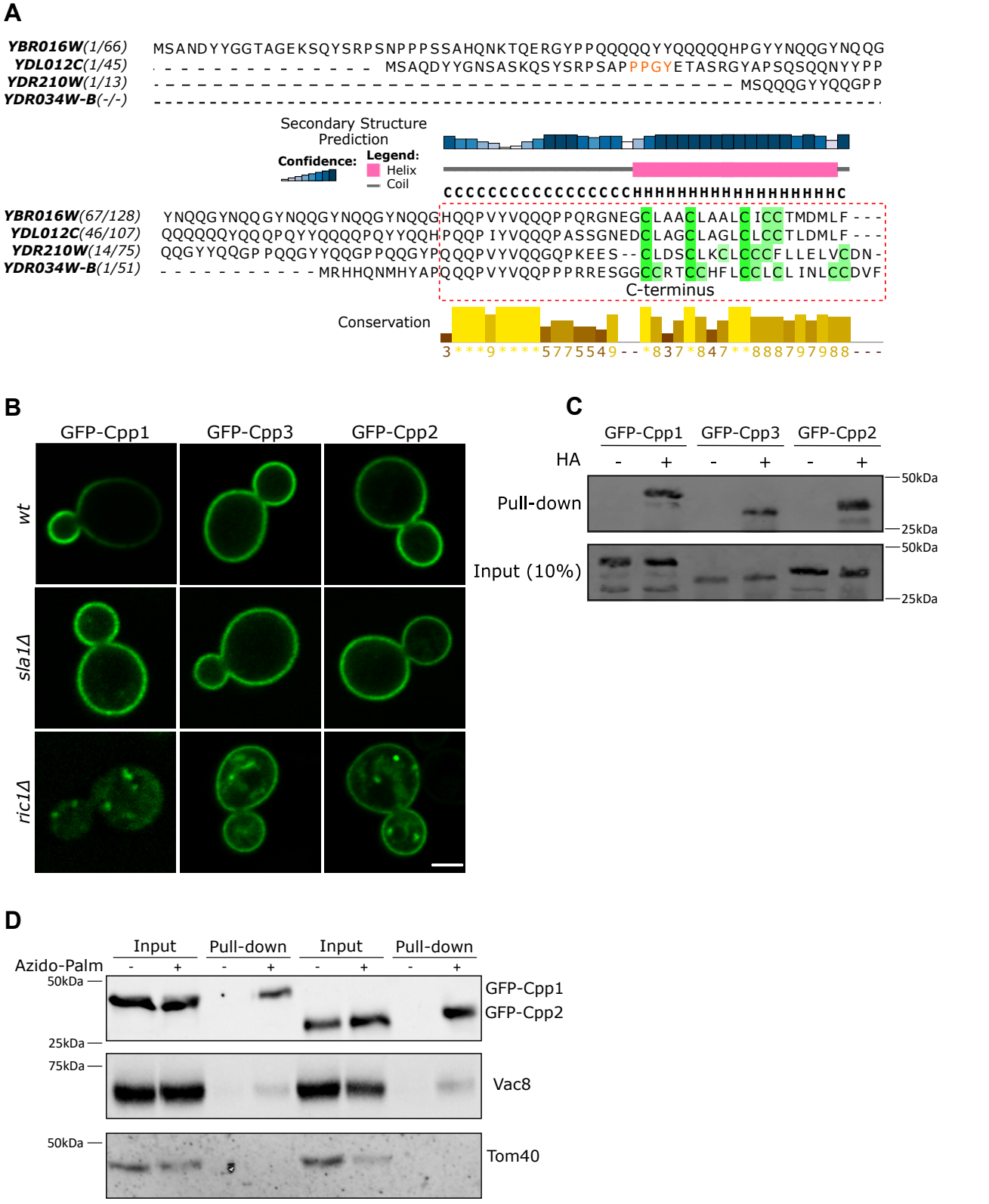

Figure 1. GFP-Cpp1, GFP-Cpp2, and GFP-Cpp3 are localized to the plasma membrane and they are palmitoylated. *A*, protein sequence alignment and secondary structure prediction for the yeast CYSPD family members. Conserved cysteines are highlighted in *green*. *B*, fluorescence images of yeast cells expressing GFP-tagged Cpp1, Cpp2, and Ccp3. The fusions localize to the plasma membrane (PM). GFP-Cpp1 is polarized to the new buds, and GFP-Cpp2 and GFP-Ccp3 are also polarized, to a lesser extent (*upper panels*). The polarized distribution of GFP-CCp1 is dependent on endocytic cycling since it is lost in a *sla1Δ* strain (*middle panels*). GFP-Cpp1 is lost from the PM in the recycling mutant *ric1Δ* and it is found in intracellular dots. GFP-Cpp2 and GFP-Cpp3 are also found inside the cell in a *ric1Δ*, but a substantial amount of fluorescence remains at the PM (*lower panels*). The scale bar represents 2 μm. *C*, acyl-biotin exchange assay on GFP-tagged Cpp1, Cpp2, and Cpp3 shows that these proteins are palmitoylated. In the hydroxylamine (HA)-treated samples, palmitates are exchanged for biotin, the proteins are pulled down using streptavidin beads and detected on a Western blot using anti-GFP antibodies. Negative

nine different transmembrane prediction software, results in just four of them suggesting the presence of a TMD. Finally, transmembrane proteins of the secretory pathway, when overexpressed, usually show some staining of the vacuole, and this was never the case for the GFP-CYSTM protein chimeras evaluated in this study. For the reasons stated above, we suspected that perhaps, these proteins are not transmembrane but are anchored to the membrane by palmitates instead. To address this issue, WT cells expressing GFP-Cpp1, GFP-Cpp2, and GFP-Cpp3 were lysed, the lysate was centrifuged at 1,00,000*g*, and the membrane fraction was treated with neutral HA, which cleaves thioester-bound palmitates. The presence of GFP-Cpp1-3 in the treated membranes and the resulting supernatants were analyzed by Western blot. Figure 2, *A* and *B* show that significant amounts of the chimeric Cpp proteins are released from the membranes and can be observed in the soluble fraction upon HA treatment. The tail-anchored transmembrane protein Tlg1 is included as a *bona fide* transmembrane protein control, and it is unaffected by the HA treatment. Other treatments that are used to release peripheral proteins from the membranes, such as high salt concentration and sodium carbonate, fail to release GFP-Cpp1 from this fraction (not shown).

As a positive control, we used GFP-Yck2, a casein kinase I homolog, that binds to membranes exclusively by palmitoylation (28). Figure 2*A* (bottom panel). However, Yck2 is aggregated *in vitro* and does not enter the gels when cells are broken by vigorous shaking with glass beads, which is how we prepared all samples. This has been carefully documented (29). On the other hand, Cpp1 and Cpp2 are quickly degraded when we try to digest the cell wall with zymolyase to prepare a protein lysate (not shown). This does not allow us to analyze both proteins in the same cells. Nevertheless, when we lyse cells–expressing GFP-Yck2 by cell wall digestion and treat membranes with HA, we can verify that the treatment is effective (Fig. 2*A*, bottom panel). Please note that the multiple bands observed for Yck2 correspond to non palmitoylated, phosphorylated, or hyperphosphorylated species (30). The highest MW band corresponds to the palmitoylated species and it is released from the pellet by HA. We have also included as a control, a non-palmitoylable GFP-Cpp1 5xΔCys lacking all cysteines. This construct behaves similarly to a GFP-Cpp1 treated with HA, that is, only a small fraction of the protein is present in the 1,00,000*g* supernatant, confirming that Cpp proteins either bind to membranes by other means or are aggregated and thus partition to the pellet fraction. Second, we placed GFP-Cpp1 under the control of the GAL1 promoter and induced the expression of the protein in the presence of 20 μM of the palmitoylation inhibitor 2-bromopalmitate (2-BP). In these conditions, the protein is observed in the cytoplasm, consistent with the behavior of a lipid-anchored protein (Fig. 2*C*). The PM SNARE Sso1, a transmembrane protein, was included as a negative control and its localization is not affected by 2-BP treatment in these conditions. As a positive control we looked at the localization of the palmitoylated protein GFP-Yck2, which changes from a PM distribution to a cytoplasmic distribution in the presence of 2-BP (Fig. 2*C*, middle panels). Finally, we sought additional evidence of the nature of the CYSTM domain by analyzing its insertion in the membrane. If the CYSTM domain is indeed a TMD, proteins bearing this domain would be tail-anchored membrane proteins, since the putative TMD is located at their C termini. Many tail-anchored proteins are inserted into the membrane with the aid of the GET complex (31). Mutant strains lacking either Get1 or Get2 show abnormal localization of tail-anchored proteins (31). Additionally, the EMC complex is involved in the insertion of low-hydrophobicity tail-anchored proteins (32, 33). Figure 3 shows that while the tail-anchored proteins Sso1 and Snc1 are mislocalized in *get1Δ* mutants, GFP-Cpp1 is unaffected. Snc1 and Sso1 are only mildly affected by the deletion of either EMC6 or EMC3, which are essential for the activity of the EMC complex. Again, GFP-Cpp1 is unaffected by the lack of either gene.

Taken together, these findings indicate the Cpp1, Cpp2, and Cpp3 and likely other CYSTM proteins are bound to membranes *via* palmitoylation and that the CYSTM domain is not necessarily transmembrane.

We, therefore, propose that this domain should be renamed to CYSPD.

CYSPD proteins are degraded in an Rsp5-dependent manner in the absence of the PATs Akr1 and Erf2

Next, we investigated whether the lack of palmitoylation has consequences in the expression or localization of the CYSPD proteins. We expressed GFP-Cpp1 in strains that each lack one of the members of the PAT family in yeast. The localization of GFP-Cpp1 was similar in a WT, *swf1Δ*, *pfa3Δ*, *pfa4Δ*, *pfa5Δ*, and *akr2Δ* strains (Fig. 4*A*). In the *erf2Δ* strain, overall fluorescence appears to be lower. However, in an *akr1Δ* strain, the fluorescence signal is completely absent (Fig. 4*A*), suggesting that GFP-Cpp1 is being degraded. There are multiple examples in the literature that highlight the link between palmitoylation and protein stability (25, 34–36). Lower levels of GFP-Cpp1 in *akr1Δ* and *erf2Δ* strains were confirmed by quantification of the fluorescence levels in these strains. The level of GFP-Cpp1 in an *erf2Δ* strain was reduced by half, and in an *akr1Δ* strain, the signal reduction is much more significant (Fig. 4*B*). GFP-Cpp2 and GFP-Cpp3 are not detectable both by fluorescence microscopy and Western blot in an *akr1Δ* strain (Fig. S1). The lack of Erf2 also affects the levels of these proteins but to different extents (Fig. S1).

Since GFP is resistant to vacuolar proteolysis in yeast and no fluorescence is observed in the vacuole, the degradation of these proteins appears to be proteasomal. Indeed, Figure 4, *C* and *D* show that degradation of GFP-Cpp1 is prevented when

controls are treated with Tris buffer instead of hydroxylamine. *D*, detection of palmitoylation by metabolic labeling and click chemistry. Yeast cells expressing GFP-Cpp1 or GFP-Cpp2 were grown in the presence (+) or absence of azido palmitate (azido-palm), lysed, and the azido palmitate was modified by biotin alkyne. Palmitoylated proteins were pulled down with streptavidin beads and analyzed by Western blot using antibodies against GFP (*upper panel*), the palmitoylated protein Vac8 (*middle panel*), or the nonpalmitoylated protein Tom40 (*lower panel*). CPP, cysteine-rich palmitoylated protein; CYSPD, cysteine-rich palmitoylated domain.

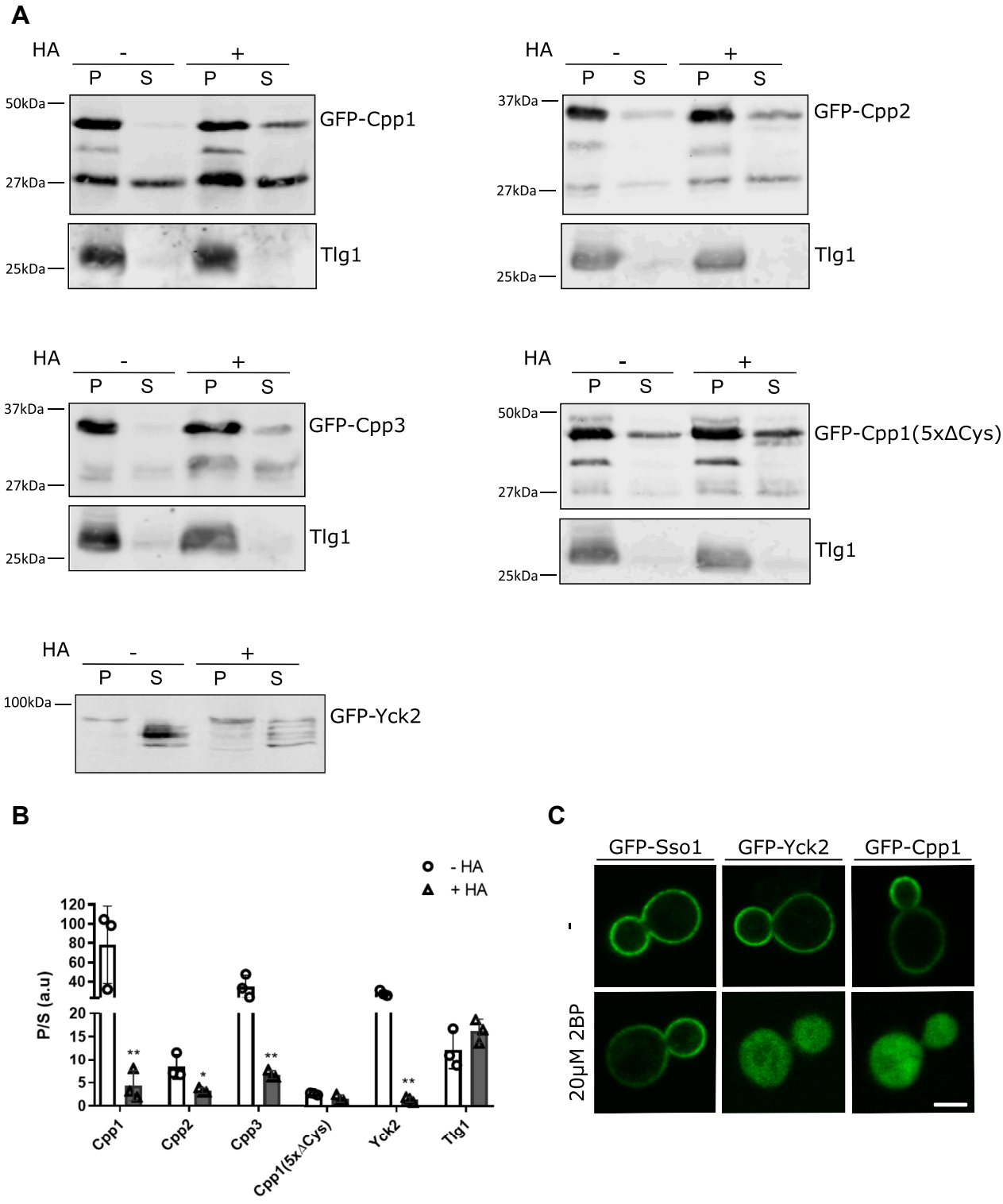

Figure 2. GFP-Cpp1, GFP-Cpp2, and GFP-Cpp3 are bound to membranes by palmitoylation. *A*, GFP-Cpp1-3 are released from membranes upon hydroxylamine treatment. Membrane fractions of yeast cells expressing GFP-Cpp1-3 were treated with 1 M hydroxylamine, which cleaves the thioester bonds between fatty acids and cysteine residues, or Tris as a control, and the presence of GFP-Cpp1 in the supernatant (S) or the membrane pellet (P) was assessed by Western blot. The endogenous transmembrane protein Tlg1 was detected in the same blots as a negative control. As positive control cells expressing GFP-Yck2 were treated as indicated above and analyzed by Western blot (*bottom left panel*). A control experiment using the non-palmitoylable version of GFP-Cpp1 (5xΔcys) was also included in the analysis (*bottom right panel*). *B*, the signals from bands as in *A* were quantified and the graph shows a *scatter plot* displaying the average pellet/supernatant (P/S) ratio ± SD for each protein from three independent experiments. *C*, fluorescence microscopy images of GFP-Cpp1 induced for 2 h by the addition of galactose, in the presence or absence of 20 μM of the palmitoylation inhibitor 2-bromopalmitate (2-BP) (*right panels*). As a negative control, Gal-driven GFP-Sso1, a transmembrane protein was included (*left panels*). Cells expressing the palmitoylated protein GFP-Yck2 were assessed as a positive control for the experiment. The scale bar represents 2 μm. CPP, cysteine-rich palmitoylated protein.

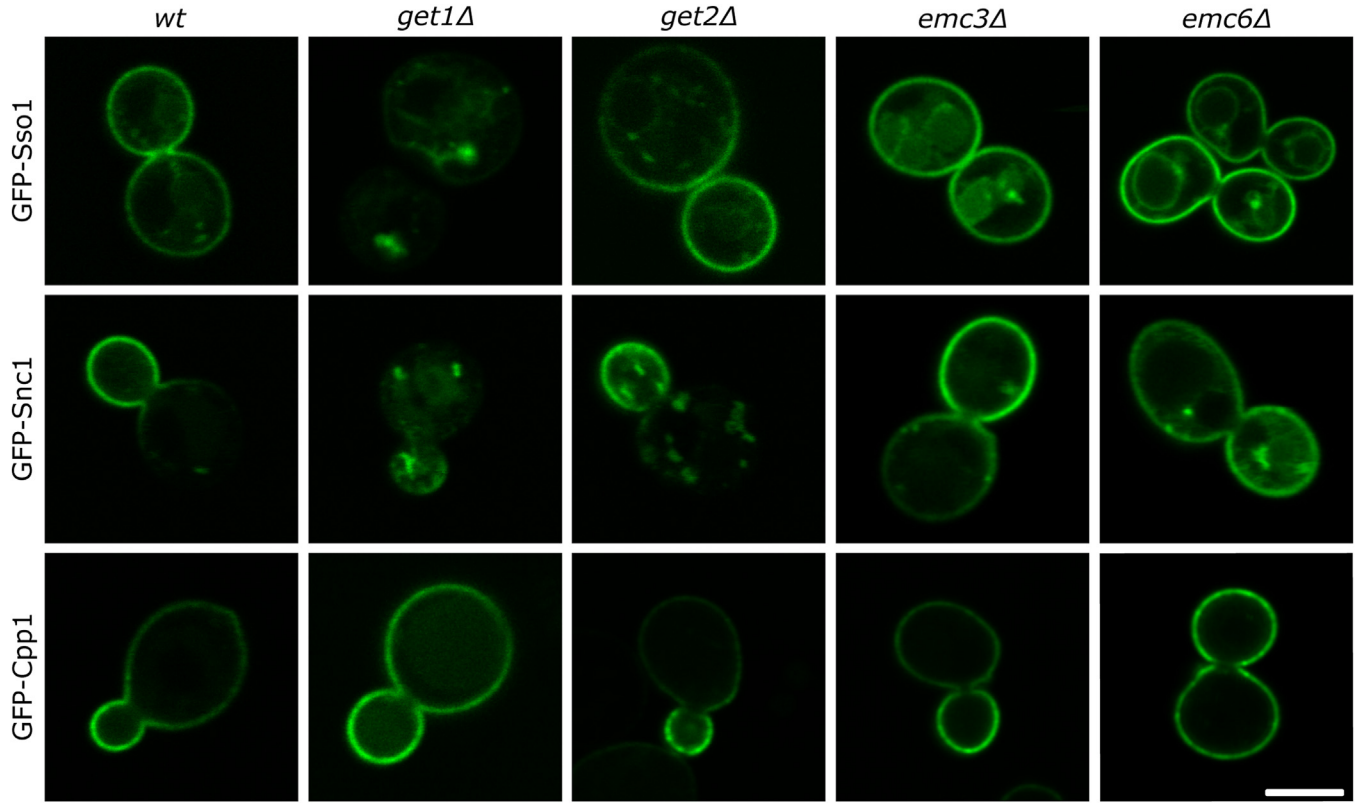

Figure 3. GFP-Cpp1 insertion in the membrane is independent of the GET and EMC complexes. Fluorescence microscopy images showing the membrane localization of GFP-Cpp1 in WT and mutant strains lacking either GET1, GET2, EMC3, or EMC6 (*lower panels*). As controls, the tail-anchored transmembrane proteins GFP-Sso1 (*upper panels*) and GFP-Snc1 (*middle panels*) were included. The scale bar represents 2 μm. CPP, cysteine-rich palmitoylated protein.

the proteasome inhibitor MG132 is added, however, the protein no longer localizes to the PM membrane, but to intracellular dots. These experiments were carried out in an *erg6Δ* genetic background, which makes the PM of these cells more permeable to drugs such as MG132 (37). These results are also consistent with the non-transmembrane nature of the CYSPD, since transmembrane proteins of the PM are mostly degraded in the vacuole.

Many proteins at the yeast PM are ubiquitinated by the ubiquitin ligase Rsp5, which controls multiple processes in the cell (38, 39). Ydl012c was found to interact with Rsp5 in a high-throughput experiment (40) and indeed, it contains a PPXY motif. These motifs are known to interact with the WW domains of ubiquitin ligases such as Rsp5 (41, 42). Since Rsp5 is an essential gene, we used a hypomorphic allele (43) (*rsp5hm*) to assess its role in the degradation of GFP-Cpp1 that takes place in an *akr1Δ* strain. We generated an *akr1Δ rsp5hm* double mutant, expressed GFP-Cpp1 and observed it under the fluorescence microscope. Figure 5*A* shows that the protein now becomes detectable, confirming the role of Rsp5 in its degradation. The rescue of GFP-Cpp1 levels in the *akr1Δ rsp5hm* was also assessed by Western blot (Fig. 5, *C* and *D*). Interestingly, GFP-Cpp1 remains localized to the PM (Fig. 5*A*, lower panel), indicating that it is either still palmitoylated by other PATs or it is anchored to the membrane by some other means. We analyzed the palmitoylation status of this protein in the *akr1Δ rsp5hm* mutant by ABE. Figure 5*B* shows that GFP-Cpp1 is palmitoylated in this double mutant, suggesting that the protein can be palmitoylated by other PAT/s when degradation is prevented. The degradation of GFP-Cpp1 in the *erf2Δ* strain is also rescued by the *rsp5hm* mutation (Fig. S2).

Mutational analyses of Cpp1 CYSPD domain

To study the palmitoylation of Cpp1 in more detail, we generated single-point mutations of the five cysteines within the CYSPD; it should be noted that no other cysteines are present in the rest of the protein. Mutants were expressed in a wild-type strain and analyzed by confocal microscopy. Fig. S3 shows that the expression levels of the single-cysteine mutants are similar to that of the wild type, and their PM localization is largely unaffected.

We next generated three additional mutant versions of GFP-Cpp1. One in which the two most N-terminal cysteines are mutated to Alanine ($C_{110,\ 114}A$). Another version in which the three most C-terminal are replaced ($C_{119,\ C121,\ 122}A$) and finally, a version in which all 5 cysteines of the domain are mutated, which we named 5xΔCys (see Fig. 6*A* for a scheme). When visualized under the microscope, all three mutants show one or two fluorescent dots in the cells, suggesting protein aggregation. Mutants ($C_{110,\ 114}A$) and $C_{119,\ C121,\ 122}A$ show

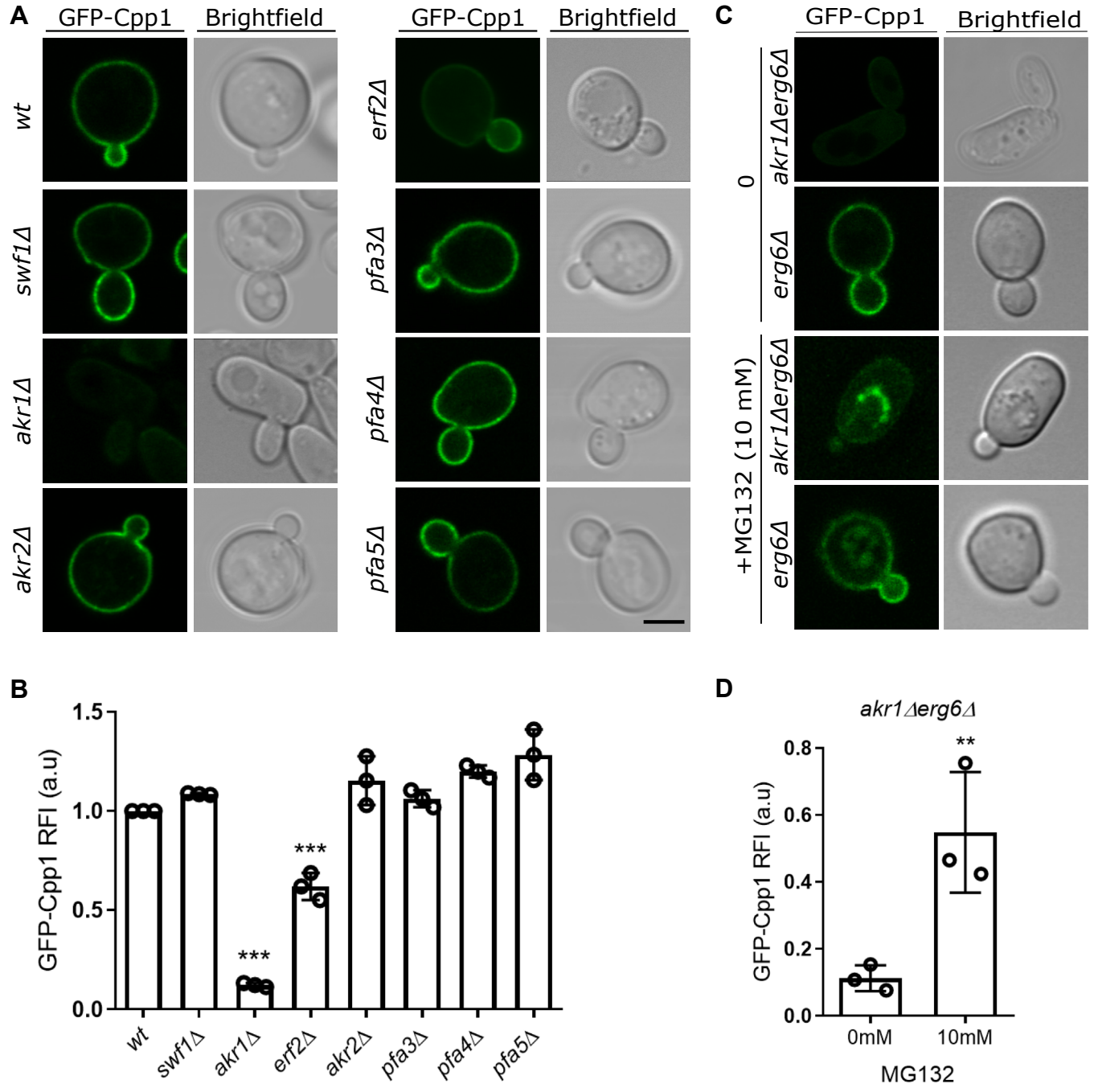

Figure 4. GFP-Cpp1 is degraded in the absence of Ark1. *A*, fluorescence microscopy images showing GFP-Cpp1 expressed in strains lacking each of the yeast PATs. Fluorescence is partially lost in *erf2Δ* and completely lost in *akr1Δ*. The scale bar represents 2 μm. *B*, the *scatter plot* graph shows the average values ± SD of the fluorescence intensity of the strains as in *A*. Total Fluorescence was measured in each cell using the same threshold for all the strains. Each average value was relativized to the average fluorescence intensity of the WT group (n = 40). *C*, fluorescence microscopy images of GFP-Cpp1 expressed in *erg6Δ* and *akr1Δ erg6Δ* strains in the presence or absence of the proteasome inhibitor MG132. Degradation of GFP-Cpp1 is prevented by the proteasome inhibitor. Experiments are carried out in an *erg6Δ* background to improve permeability to the drug. The scale bar represents 2 μm. *D*, *scatter plot* graph showing the fluorescence intensity average ± SD of GFP-Cpp1 in the double mutant *akr1Δ erg6Δ* strain, measured in the presence or absence of MG132. Each average value was relativized to the average fluorescence intensity of the control cells *erg6Δ* (n = 20). a. u: arbitrary units; CPP, cysteine-rich palmitoylated protein; PAT, palmitoyltransferase; RFI, relative fluorescence intensity.

some remaining fluorescence on the PM (Fig. 6*C* bottom panels) while the 5xΔCys mutant has no remaining fluorescence on the membrane. When the palmitoylation of these mutants was tested using an ABE assay, it was observed that, as expected, the 5xΔCys mutant is not palmitoylated, however, both ($C_{110,\ 114}$A) and ($C_{119,\ C121,\ 122}$A) are, suggesting that cysteines in both halves of the domain can be palmitoylated (Fig. 6*D*). Importantly, if the CYSPD was indeed a TMD, cysteines 119, 121 and 122 would be expected to be buried deep into the membrane and could not be palmitoylated. This

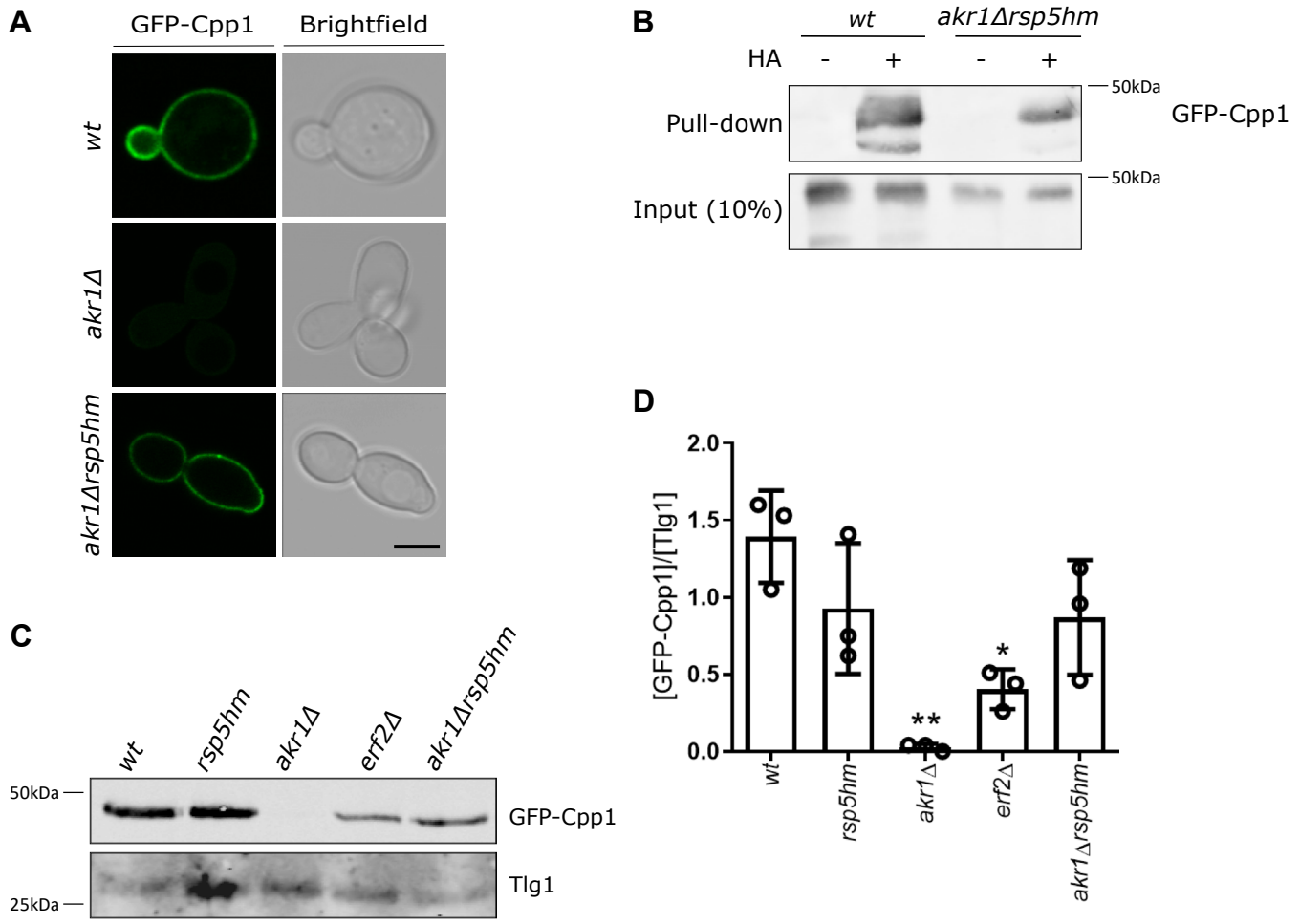

Figure 5. GFP-Cpp1 degradation is dependent on Rsp5. *A*, fluorescence microscopy images of GFP-Cpp1 expressed in WT (*upper panel*), *akr1Δ* (*middle panel*), and *akr1Δ rsp5hm* (*lower panel*) strains. In the absence of Akr1, the expression and localization of GFP-Cpp1 are rescued by lowering the levels of Rsp5. The scale bar represents 2 μm. *B*, acyl-biotin exchange assay of GFP-Cpp1 expressed in WT and *akr1Δ rsp5hm* strains, showing that the protein remains palmitoylated when degradation is precluded. *C*, Western blot analysis showing the expression levels of GFP-Cpp1 in WT and indicated mutant strains. GFP-Cpp1 is partially degraded in *erf2Δ*, completely degraded in *akr1Δ* and this degradation is partially precluded in *akr1Δ rsp5hm* strain. Tlg1 was used as a loading control. *D*, bar graph showing the average values ± SD from the quantification of three independent experiments as in C. CPP, cysteine-rich palmitoylated protein; CYSPD, cysteine-rich palmitoylated domain; HA, hydroxylamine.

is due to the cytosolic localization of the catalytic domains of PATs (44).

Palmitoylation dependent and palmitoylation independent degradation of GFP-Cpp1

Interestingly, none of the cysteine mutants of GFP-Cpp1 described above fully recapitulates the complete degradation triggered by the loss of Akr1, nor the partial degradation, while still maintaining membrane localization, that is observed in *erf2Δ*. It is possible that the absence of palmitoylation due to the lack of a PAT, which leaves free cysteine residues in the substrate, is not strictly equivalent to having no palmitoylation caused by point mutations in the cysteines (25). Alternatively, the lack of Akr1 and Erf2 could have an indirect effect on the half-life of these proteins. To assess this point, we generated constructs in which we either truncated the CYSPD domain of Cpp1, (Cpp1-ΔCYSPD) or replaced it with the TMD of Sso1 (Cpp1-Sso1) and we expressed them in *wild type* and a*kr1Δ* strains along with Cpp1-5xΔCys. Figure 7*A* indicates that when GFP-Cpp1 Cpp1-5xΔCys and Cpp1-ΔCYSPD are expressed in an a*kr1Δ* strain, they are completely degraded, suggesting that loss of Akr1 can affect GFP-Cpp1 stability independently of its palmitoylation. On the other hand, Cpp1-Sso1 seems to be protected from degradation in an a*kr1Δ* strain.

A similar experiment was carried out in an *erf2Δ* mutant. In this case, the loss of the PAT resulted in diminished levels of GFP-Cpp1 as expected (Fig. 7*B*), but the degradation of mutants lacking the palmitoylation region (CYSPD) is no longer enhanced by the lack of Erf2. Cpp1-Sso1 is also expressed at higher levels in the WT strain and a decrease in the level of Cpp1-Sso1 TMD is observed in the mutant, suggesting that perhaps the stability of the construct is affected by the lack of Erf2, indirectly.

Overall, these results suggest that the loss of stability GFP-Cpp1 in an *erf2Δ* is likely due to diminished palmitoylation, while the loss of stability observed in *akr1Δ* mutants is mostly due to an indirect effect. However, palmitoylation of CYSPD domains by Akr1 cannot be discarded.

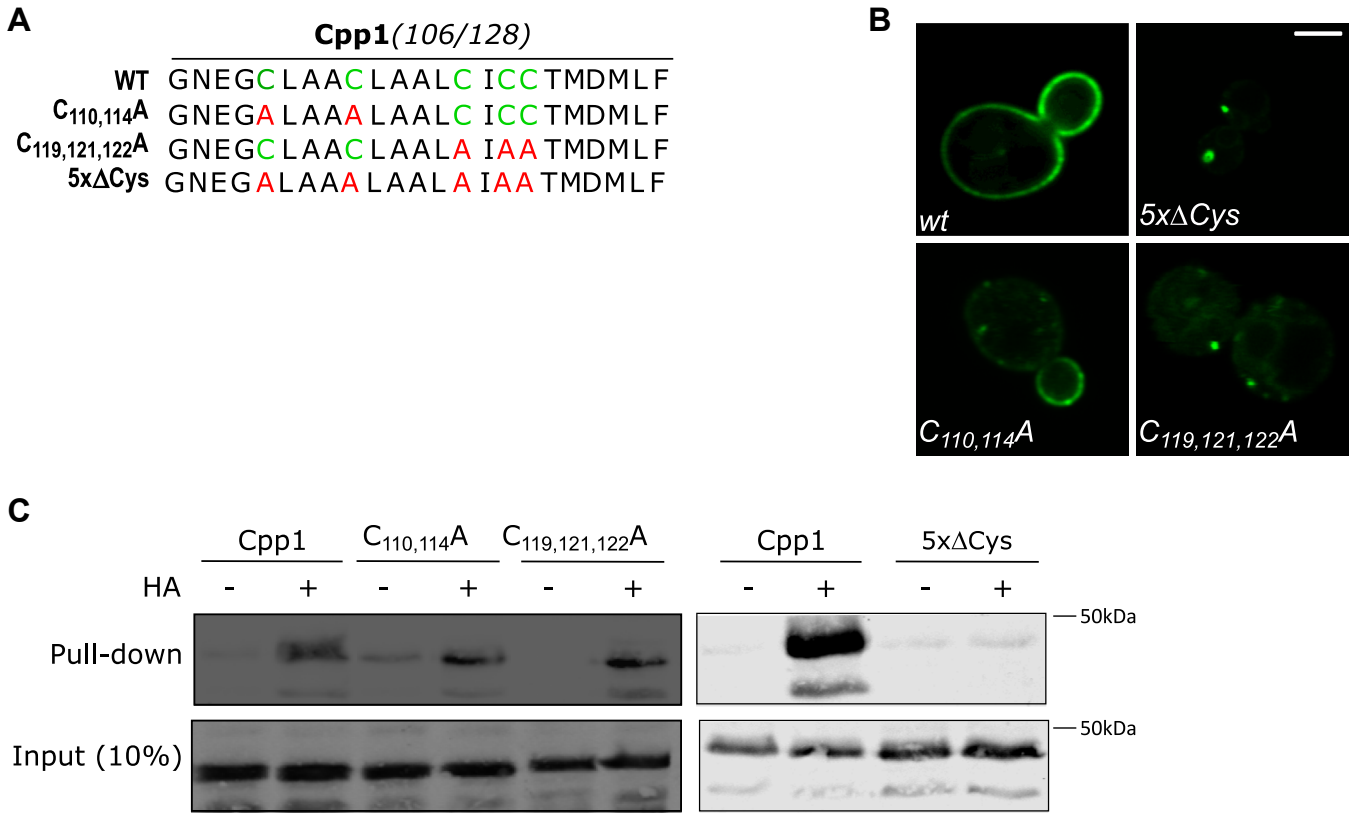

Figure 6. Palmitoylation and localization of GFP-Cpp1 cysteine mutants. *A*, amino acid sequences of WT and cysteine mutants in Cpp1 CYSPD. Cysteines are colored in *green* and introduced alanines are colored in *red*. *B*, fluorescence microscopy images of GFP-Cpp1 and the GFP Cpp1 cysteine mutants. The scale bar represents 2 μm. *C*, acyl-biotin exchange (ABE) assay of WT GFP-Cpp1 and indicated cysteine mutants, showing that cysteines in both halves of the domain can be palmitoylated. CPP, cysteine-rich palmitoylated protein; CYSPD, cysteine-rich palmitoylated domain; HA, hydroxylamine.

Discussion

In this work we have begun the characterization of a family of small proteins for which very little is known at the molecular and cell biological level. We showed that three of the four members of the CYSTM family of proteins are palmitoylated and that the domain is unlikely to be transmembrane, hence we suggest that the domain be renamed to CYSPD. Since some of the cysteines present in this domain are conserved, likely, homologs from other species will also be palmitoylated. Moreover, we have preliminary data indicating the Mnc1, the Cpp3 paralog, although not strictly a CYSTM protein, is also palmitoylated although it might bind to membranes differently. This highlights the need for a reassessment of the CYSTM/CYSPD family definition even further. More research is required to advance in this direction.

GFP tagging and microscopy have confirmed high-throughput data indicating that Cpp1, Cpp2 and Cpp3 are localized to the PM in a polarized manner. We show that this polarization depends on endocytosis and recycling. However, they are polarized to different extents, suggesting different efficiencies of their endocytosis signals or different rates of diffusion. It might be interesting to investigate this matter further. Perhaps, these different diffusion rates might be due to different palmitoylation patterns, that is, either more cysteines being palmitoylated or having different occupancies.

Reports both in yeast (3) and in plants (9) suggested localizations other than the PM for some members of the CYSPD family. However, in both cases, proteins were tagged with GFP at the C terminus. Since the CYSPD is responsible for membrane binding, tagging in this region may interfere with the protein's localization. However, the CYSTM family is large and localizations other than the PM cannot be excluded.

We also present several lines of evidence to suggest that the CYSTM-containing proteins in yeast are not transmembrane as previously suggested (1) but instead are bound to membranes *via* S-acylation. The most direct strategy to demonstrate binding to the membranes *via* palmitoylation is to cleave the thioester bond by incubation with neutral HA. We showed that upon treatment of membrane fractions with this reagent, a significant amount of GFP-Cpp1-3 is released into the soluble fraction. The release is not complete, and this might be due to non-palmitoylated proteins being aggregated *in vitro*. This is consistent with the behavior of GFP-Cpp1 5xΔCys, which is also partially present in the soluble fraction; however, we cannot exclude other factors that may be keeping the proteins attached to membranes such as interacting partners. The non-transmembrane, palmitoylated protein SNAP25 can maintain membrane association in the absence of S-acylation (45). Nevertheless, *bona fide* transmembrane proteins such as Tlg1 are not released from the membranes by treatment with HA.

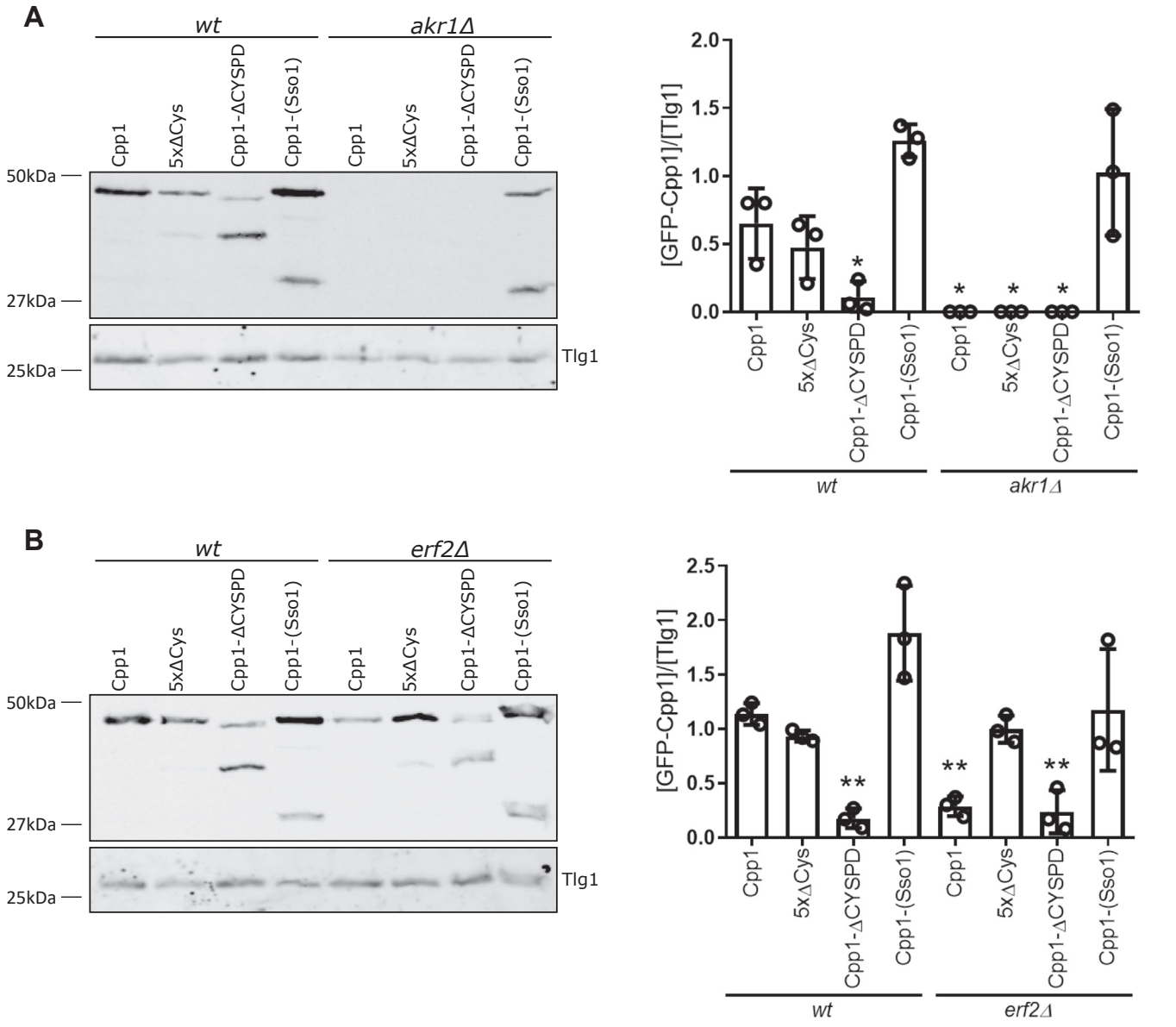

Figure 7. Degradation of GFP-Cpp1 in *akr1Δ* is independent of the CYSPD domain. *A*, Western blot analysis of GFP-Cpp1 and mutant versions with either all the cysteines mutated to alanine (5xΔCys), lacking the CYSPD domain (ΔCYSPD) or with the CYSPD replaced by the transmembrane domain of Sso1 Cpp1-(Sso1), were expressed in WT and *akr1Δ* strains (*left panel*). The band intensities were quantified and graphed. Plots show the mean values ± SD from three independent experiments (*right panel*). *B*, Western blot analysis of GFP-Cpp1 and mutant versions with either all the cysteines mutated to alanine (5xΔCys), lacking the CYSPD domain (ΔCYSPD) or with the CYSPD replaced by the transmembrane domain of Sso1 Cpp-(Sso1), were expressed in WT and *erf2Δ* strains (*left panel*). The band intensities were quantified and graphed. Plots show the mean ± SD values from three independent experiments (*right panel*). Tlg1 was used as a loading control. CPP, cysteine-rich palmitoylated protein; CYSPD, cysteine-rich palmitoylated domain.

The second line of evidence is provided by the treatments with the palmitoylation inhibitor 2-BP. At low concentrations of this drug, we can see that GFP-Cpp1 is greatly affected, exhibiting some puncta and some soluble distribution, as is the positive control GFP-Yck2, while the negative control protein GFP-Sso1 is not. A higher concentration of 2-BP grossly affects the GFP-Sso1 control (not shown). This is to be expected since 2-BP is a very toxic inhibitor, known to affect multiple processes in the cell including membrane traffic (reviewed in (13)).

Additional, indirect evidence for the non-transmembrane nature of these proteins stems from the fact that they are degraded *via* the proteasome since degradation is stopped by the addition of MG132, while most transmembrane proteins of the late secretory pathway are degraded in the vacuole.

If these proteins were tail-anchored transmembrane proteins, they should be inserted in the ER membrane by the GET complex (31) or the EMC complex (32, 33). Deletion of GET2 shows a striking effect on the localization of the tail-anchored proteins Sso1 and Snc1, while GFP-Cpp1 distribution remains completely unaffected, in these conditions or the absence of a functional EMC complex.

Finally, a compelling argument for the non-transmembrane nature of these proteins is the fact that when cysteines 110 and 114 are absent from the GFP-Cpp1 construct, the protein remains palmitoylated. The TMD model for Cpp1 CYSPD (1)

indicates that the remaining cysteines (119, 121, and 122) would be buried deep into the membrane and hence not available for palmitoylation (46, 47). Cysteine 119, the closest to the cytoplasmic border available for palmitoylation in the $C_{110\ 114}A$ double mutant is predicted to be in position 12 from the cytosolic border (see Fig. 1*A*). We have also analyzed a triple mutant $C_{110\ 114\ 119}A$ and the protein remains palmitoylated (not shown). This would be very unlikely if the CYSPD was indeed a transmembrane domain.

We next assessed the effect of the absence of individual yeast PATs on GFP-CYSPD proteins. We found a striking effect of deleting AKR1. The lack of this PAT led to the complete degradation of all CYSPD proteins analyzed. The deletion of ERF2 led to a partial degradation of Cpp1 and Cpp3. Degradation was far more pronounced for Cpp2.

Interestingly, when palmitoylation of Cpp1 is abolished by mutation of the cysteines, the protein forms aggregates inside the cell but it can be detected both by microscopy and Western blot. One possibility to explain this is that losing palmitoylation of a particular cysteine by deletion of Akr1 generates an incompletely palmitoylated species, which is more unstable than a mutant lacking all palmitates due to cysteine mutations. However, this does not appear to be the case, since single-cysteine mutants and a combination of double and triple mutants expressed in a WT strain, never recapitulate the complete degradation observed in *akr1Δ*. This led us to hypothesize that the loss of Akr1 might have an effect that is independent of the presence of a CYSPD domain and hence its palmitoylation status. We demonstrated this effect using constructs that either lacked the CYSPD domain or that had all the cysteines mutated to alanine and comparing the protein levels in WT and *akr1Δ* strains. The effect of the lack of Akr1 on the stability of CYSPD proteins is intriguing. Akr1 has multiple substrates (14) and the loss of this protein leads to diminished growth and morphological phenotypes (30). The metabolic state generated by the loss of this protein may be sensed by the cytoplasmic domains of CYSPD proteins, triggering their degradation. This might in the future lead to clues on the molecular function of CYSPD proteins. The effect could be due to either loss of function of a palmitoylated Akr1 substrate or gain of function of the nonpalmitoylated (or abnormally) palmitoylated substrate (or both), so a simple deletion analysis of Akr1 substrates might not be able to identify which Akr1 substrate is responsible. One way to single out Akr1 substrates involved in Cpps degradation is to use versions of these substrates whose palmitoylation is independent of Akr1, so they can remain "active" in its absence. One interesting candidate is Yck2, a casein kinase I homolog, involved in morphogenesis, proper septin assembly, endocytic trafficking, and glucose sensing (48, 49). We expressed Cpp1 in the strain NDY1953. This strain has a palmitoylation-independent allele of Yck2 (30) in which Yck2 can bind to membranes since it bears the C-terminal domain of Ras2, which is prenylated, and later palmitoylated by Erf2. In this strain, Cpp proteins are still completely degraded, suggesting that processes downstream Yck2 are not involved in Cpp1 degradation (not shown). Another interesting candidate is the Sphingoid long-chain base kinase Lcb4, responsible for the synthesis of long-chain base phosphates. The localization of this protein is dependent on Akr1 (50). Long-chain base phosphates in yeast are signaling molecules involved in multiple cellular processes, including resistance to heat-stress and Ca2+ mobilization (51, 52).

The degradation of Cpp proteins mediated by the loss of Erf2 is, on the other hand, likely related to incomplete palmitoylation of the CYSPD.

We have shown that the ubiquitin ligase Rsp5 has a role in the degradation of CYSPD proteins, which may lead to significant insights into the molecular function of these proteins.

Our mutational analysis indicates that no single cysteine is crucial for stability, suggesting that more than one cysteine is palmitoylated in the steady state. The double and triple mutants analyzed in Figure 6*C* indicate that at least two cysteines are modified. We carried out acyl-PEG exchange experiments to try to resolve this issue. In this technique, palmitates are exchanged by five kDa PEG molecules, leading to shifts in the molecular weight, for each palmitoylated cysteine. We found shifts that corresponded to either two palmitoylated cysteines and a more minoritarian shift, indicating four palmitoylated cysteines (not shown). However, we are not confident that cysteines that are next to each other in a sequence can be efficiently detected by this technique due to steric hindrance. A definitive model for the steady-state palmitoylation of CYSPD proteins will require specialized mass spectrometry studies and a detailed mutagenic analysis of the domain.

The molecular mode of action of these proteins remains mysterious; it has been hypothesized that the cysteines present in the domain would chelate metals (1, 2). However, some or most of these cysteines are likely palmitoylated and therefore unavailable for the chelation of metals. The mechanisms by which these proteins may contribute to resistance to stress caused by metals remain to be uncovered. A deeper understanding of these proteins' topology is a first and necessary step toward understanding their function.

Experimental procedures

Plasmids and strains

BY4741 (*MATa his3Δ1 leu2Δ0 met15Δ0 ura3Δ0*) strain and its derivatives, *sla1Δ, ric1Δ, erg6Δ, get2Δ, get3Δ, emc6Δ, emc3Δ, swf1Δ, pfa3Δ, pfa4Δ, pfa5Δ, erf2Δ, akr1Δ, and akr2Δ* are from the EUROSCARF consortium. The *rsp5* hypomorph *rsp5hm* (EN44) strain was a gift from Dr Hugh Pelham (MRC Lab. of Molecular Biology). The *rsp5hm/akr1Δ* strain was generated by crossing the single mutant strains and selection of recombinant haploid double-mutant progeny. The *akr1Δ erg6Δ* was described in (53). *erf2Δ rsp5hm* was derived from *rsp5hm* transformed with an ERF2 deletion cassette. The cassette was amplified from a PCRscript plasmid containing *S. pombe* HIS5 with oligos oErf2 KO3 and oErf2 KO5. The deletion was verified by PCR using oligos oErf2 02 and oErf2 06. See Table S1 for a list of the oligonucleotides used throughout this work.

Expression of the N-terminal GFP-tagged CYSPD proteins was carried out from pRS416-based plasmids containing the

TPI1 promoter and Pep12 terminator. To generate GFP-Cpp1 cysteine mutants, we first introduced a *Hind*III site upstream of the CYSPD (PJV480). To generate the GFP-Cpp(C110A), the region coding for the C-terminal domain of Cpp1 followed by the PEP12 terminator was amplified using oligos oYbr016w 03 and oYbr016w 06. This fragment was digested *Hind*III/*Xba*I and cloned in PJV850 in the same sites. The mutant Cpp1(C110A) generated was digested *Eco*RI/*BamH*I and the fragment was cloned into PJV3 plasmid in the same sites (PRS416-based vector used to express N-terminal GFP tagged proteins under TPI promoter control). To generate the GFP-Cpp1(C114A) the region coding for its CYSPD followed by the PEP12 terminator was amplified using oligos oYbr016w 04 and oPep12TR. This fragment was digested HindIII/XbaI and was cloned in PJV850 in the same sites. The mutant ORF was digested EcoRI/BamHI and the fragment was cloned into PJV3 in the same sites. To generate GFP-Cpp1(C121A) the ORF was amplified using oligos oYbr016w 01 and oYbr016w 08. This fragment was digested *Eco*RI/*Bam*HI and was cloned into PJV3 in the same sites. To generate the GFP-Cpp1(C122A) the ORF was amplified using oligos oYbr016w 01 and oYbr016w 09. This fragment was digested *Eco*RI/*Bam*HI and was cloned into PJV3 in the same sites. To generate the GFP-Cpp1(C110,114A) the region coding for its CYSPD domain followed by the PEP12 terminator was amplified using oligos oYbr016w 05 and oYbr016w 06. This fragment was digested *Hind*III/*Xba*I and was cloned in PJV850 in the same sites. The double mutant generated was digested *Eco*RI/*Bam*HI and the fragment was cloned into PJV3 in the same sites. To generate the GFP-Cpp1(C119, 121, 122A) the Cpp1 ORF was amplified using oligos oYbr016w 05 and oYbr016w 10. This fragment was digested with *Eco*RI/*Bam*HI and was cloned into PJV3 in the same sites. To generate the GFP-Ybr016wΔCYSPD the ORF of Cpp1 was amplified using oligos oYbr016w 01 and oYbr016w 11. This fragment was digested *Eco*RI/*Bam*HI and was cloned into PJV3 in the same sites. To generate GFP-Cpp1(Sso1) the ORF was amplified using oligos oYbr016w 01 and oYbr016w 12. This fragment was digested *Eco*RI/*Hind*III and was cloned in PJV481 (described in (54). The chimera Cpp1(Sso1) was digested *Eco*RI/*Bam*HI and cloned into PJV3.

Bioinformatics

The protein sequences of Cpp1, Ydl012c, Cpp2, and Cpp3 were downloaded and Clustal Omega (55) was used to perform the alignment. The alignment was manually curated and refined using Jalview (56). For secondary structure prediction of each protein, PSIPRED 4.0 (57) was used.

Yeast fluorescence microscopy

Cells expressing GFP fusions were grown overnight, diluted to 0.1 OD ml, and grown for 3 to 4 h. Cells were imaged live with an Olympus FV1200 confocal microscope equipped with PLAPON60 × oil SC21.4 numerical aperture objective. All microscopy images were processed with the software FIJI from NIH (58) (https://fiji.sc/).

Proteasome inhibition with MG132

GFP-Cpp1 was expressed under the control of the GAL1 promoter. Cells were grown overnight in lactate as the sole carbon source, diluted and induced for 3 h in a medium containing galactose 2%. Before visualization, the cells were washed with a medium containing glucose to repress the expression of GFP-Cpp1. MG132 was added to a final concentration of 10 μM for 1 h and cells were observed live under the microscope.

SDS-page and Western blot

Total protein extracts were prepared as follows: To media containing 10 OD of yeast cells at OD = 1 trichloro acetic acid was added to a final concentration of 10% v/v. The mixture was incubated for 10 min on ice, then centrifuged for 2 min at 10,000*g*, and the supernatant was removed. The pellet was resuspended in 300 μl of 10% V/V trichloro acetic acid and 200 μl of 0.5 mm diameter glass beads were added. Cells were mechanically lysed by vigorous shaking three times for 3 min at 4 °C using Disruptor Genie (Scientific Industries) incubating for 2 min on ice, between each shaking. The samples were centrifuged for 1 min at 300*g* to remove glass beads and cell debris. Proteins were precipitated by centrifugation for 1 min at 16,000*g*. The supernatant was discarded, and the pellet was resuspended in 45 μl of SDS sample buffer with 20% 2-β mercaptoethanol and 5 μl of 1 M Tris base to neutralize excess acidity. The samples were heated for 5 min at 95 °C submitted to SDS-PAGE.

Antibodies: mouse monoclonal anti-GFP was from ROCHE Life Sciences, (11814460001500). Polyclonal anti-Vac8 antibodies were kindly supplied by Dr Christian Ungermann anti-Tlg1 antibodies were a gift from Dr Hugh Pelham. The blots were probed using secondary antibodies IRDye 680 or IRDye 800 (Li-Cor bioscience UK, 51-926-32210; 1:20,000) and then scanned using an Odyssey Infrared scanner (Li-Cor bioscience). The intensity of the bands was quantified using ImageJ software (https://imagej.net/ij/).

Acyl-biotin exchange

The ABE method was carried out as described in (53).

Metabolic labeling and click chemistry

Cells were grown in YPAD media to logarithmic phase 25 μM palmitic acid-azide (15-azidopentadecanoic acid) (Thermo Fisher Scientific; labeled) for 2 h in the dark. Control samples were incubated with dimethyl sulfoxide instead (unlabeled). Ten A_{600} units of cells were harvested for each condition and resuspended with 300 μl buffer (50 mM Tris pH = 8, 1% SDS, 1 mM PMSF, protease inhibitor cocktail containing 0.1 mg/ml leupeptin, 0.5 mg/ml pepstatin A, 0.1 mM Pefabloc). One hundred microliters of acid-washed beads were added and cells were mechanically lysed twice in a FastPrep device (6 m/s for 40 s; MP Biomedicals), with a 5-min incubation on ice in between. The cell lysate was centrifuged at 20,000*g* for 20 min and 4 °C. Fifty microliters of lysate were used to perform click-chemistry labeling using the Click-iT

Protein Reaction Buffer Kit (Thermo Fisher Scientific) according to the manufacturer's instructions, with 40 μM biotin alkyne (PEG4 carboxamide-propargyl biotin) (Thermo Fischer Scientific) as the detection reagent. After chloroform-methanol precipitation of the proteins, the pellet was resuspended in 100 μl of resuspension buffer (4% SDS, 50 mM Tris–HCl pH 7.4, 5 mM EDTA), and 5 μl were removed as the input sample. One milliliter of dilution buffer (50 mM Tris–HCl pH 7.4, 5 mM EDTA, 150 mM NaCl, 0.2% Triton X-100) was added to the sample, and it was combined with 30 μl of slurry of prewashed high-capacity streptavidin beads (Thermo Fisher Scientific). The sample and beads were incubated for 1 h at room temperature with end-over-end rotation. The beads were washed three times with dilution buffer. The proteins were eluted by the addition of 40 μl of sample buffer (250 mM Tris–HCl pH:8, 8% SDS, 40% glycerol, 0,04% BPB) with β-mercaptoethanol and heating at 95 °C for 10 min. The samples were analyzed by SDS-PAGE and Western blot.

Subcellular fractionation and HA treatment

Thirty *A* units of cells at *A* = 1 were lysed by glass bead disruption in lysis buffer (50 mM Tris buffer pH 7.4, 5 mM EDTA, 150 mM NaCl, and 10 mm N-ethylmaleimide). The lysate was centrifuged for 4 min at 300*g* and then the supernatant was centrifuged for 20 min at 17,000*g* to collect the membrane fraction. This pellet was resuspended in 300 μl of lysis buffer with a tuberculin syringe. Half of the sample was treated with 1M HA pH7 and the remaining half with 1M neutral Tris buffer as control. The samples were incubated with rotation for 3 h at room temperature and then centrifuged for 30 min at 17,000*g*. The supernatants were transferred to a new tube and proteins were precipitated with chloroform: methanol, air-dried, and resuspended in sample buffer (4% SDS, 50 mm Tris–HCl pH 7.4, 5 mm EDTA). The pellets were resuspended in 300 μl of lysis buffer, Triton X-100 was added to 1.7% final concentration, and the samples were incubated with rotation for 30 min at 4 °C. After a brief centrifugation the supernatant was collected as a membrane fraction. Proteins were precipitated with chloroform: methanol and resuspended in sample buffer.

Statistical analysis

Results are presented as scatter plots, reporting means ± SD. Statistical analyses were performed using ANOVA with GraphPad Prism 5.00 software (https://www.graphpad.com/features). Significance (*) was attributed to the 95% level of confidence ($p < 0.05$)

Data availability

Most data are contained within the manuscript. Experiments labeled as "not shown" or "preliminary," are available upon request. Contact javier.valdez@unc.edu.ar.

Supporting information—This article contains supporting information.

Acknowledgments—We thank Ayelen Gonzalez Montoro for critical reading of the manuscript, Maya Schuldiner and Emma Fenech for suggesting the Emc3 and Emc6 controls, and finally Hugh Pelham, for pointing us in the direction of these "Funny Little proteins."

Author contributions—M. L. G., G. B., and R. M. investigation; M. L. G. and G. B. visualization; M. L. G., G. B., and J. V. T. writing-review and editing; J. V. T. supervision; J. V. T. writing-original draft; J. V. T. funding acquisition; J. V. T. project administration.

Funding and additional information—This work was supported by the Secretaría de Ciencia y Tecnología, Universidad Nacional de Córdoba and by Agencia Nacional de Promoción Científica y Tecnológica, Argentina (grant PICT 2017 1709 and PICT 2020 0397 to J. V. T). R. M. and M. L. G. have fellowships from CONICET. J. V. T. is a Career Investigator of CONICET (Argentina).

Conflict of interest—The authors declare that they have no conflicts of interest with the contents of this article.

Abbreviations—The abbreviations used are: 2-BP, 2-bromopalmitate; ABE, acyl-biotin exchange; CPP, cysteine-rich palmitoylated protein; CYSPD, cysteine-rich palmitoylated domain; CYSTM, cysteine-rich transmembrane; HA, hydroxylamine; Mnc, manganese-chelating protein; PAT, palmitoyltransferase; PM, plasma membrane; TMD, transmembrane domains.

References

1. Venancio, T. M., and Aravind, L. (2010) CYSTM, a novel cysteine-rich transmembrane module with a role in stress tolerance across eukaryotes. *Bioinformatics* **26**, 149–152
2. Andreeva, N., Kulakovskaya, E., Zvonarev, A., Penin, A., Eliseeva, I., Teterina, A., *et al.* (2017) Transcriptome profile of yeast reveals the essential role of PMA2 and uncharacterized gene YBR056W-A (MNC1) in adaptation to toxic manganese concentration. *Metallomics* **9**, 175–182
3. Zvonarev, A., Ledova, L., Ryazanova, L., Valiakhmetov, A., Farofonova, V., and Kulakovskaya, T. (2023) The YBR056W-A and its ortholog YDR034W-B of S. cerevisiae belonging to CYSTM family participate in manganese stress overcoming. *Genes (Basel)* **14**, 987
4. Beilharz, T., Egan, B., Silver, P. A., Hofmann, K., and Lithgow, T. (2003) Bipartite signals mediate subcellular targeting of tail-anchored membrane proteins in Saccharomyces cerevisiae. *J. Biol. Chem.* **278**, 8219–8223
5. Huh, W. K., Falvo, J. V., Gerke, L. C., Carroll, A. S., Howson, R. W., Weissman, J. S., *et al.* (2003) Global analysis of protein localization in budding yeast. *Nature* **425**, 686–691
6. Lee, J. K., Kim, M., Choe, J., Seong, R. H., Hong, S. H., and Park, S. D. (1995) Characterization of uvi15+, a stress-inducible gene from Schizosaccharomyces pombe. *Mol. Gen. Genet.* **246**, 663–670
7. Kuramata, M., Masuya, S., Takahashi, Y., Kitagawa, E., Inoue, C., Ishikawa, S., *et al.* (2009) Novel cysteine-rich peptides from Digitaria ciliaris and Oryza sativa enhance tolerance to cadmium by limiting its cellular accumulation. *Plant Cell Physiol.* **50**, 106–117
8. Sauerbrunn, N., and Schlaich, N. L. (2004) PCC1: a merging point for pathogen defence and circadian signalling in Arabidopsis. *Planta* **218**, 552–561
9. Xu, Y., Yu, Z., Zhang, D., Huang, J., Wu, C., Yang, G., *et al.* (2018) CYSTM, a novel non-secreted cysteine-rich peptide family, involved in environmental stresses in arabidopsis thaliana. *Plant Cell Physiol.* **59**, 423–438
10. Joshi, J. R., Singh, V., and Friedman, H. (2020) Arabidopsis cysteine-rich trans-membrane module (CYSTM) small proteins play a protective role mainly against heat and UV stresses Funct. *Plant Biol.* **47**, 195–202
11. Mastrokolias, A., Ariyurek, Y., Goeman, J. J., van Duijn, E., Roos, R. A., van der Mast, R. C., *et al.* (2015) Huntington's disease biomarker

progression profile identified by transcriptome sequencing in peripheral blood. *Eur. J. Hum. Genet.* **23**, 1349–1356
12. Mitchell, D. A., Vasudevan, A., Linder, M. E., and Deschenes, R. J. (2006) Protein palmitoylation by a family of DHHC protein S-acyltransferases. *J. Lipid Res.* **47**, 1118–1127
13. Chamberlain, L. H., and Shipston, M. J. (2015) The Physiology of protein S-acylation. *Physiol. Rev.* **95**, 341–376
14. Roth, A. F., Wan, J., Bailey, A. O., Sun, B., Kuchar, J. A., Green, W. N., *et al.* (2006) Global analysis of protein palmitoylation in yeast. *Cell* **125**, 1003–1013
15. Gonzalez Montoro, A., Chumpen Ramirez, S., Quiroga, R., and Valdez Taubas, J. (2011) Specificity of transmembrane protein palmitoylation in yeast. *PLoS One* **6**, e16969
16. Smotrys, J. E., and Linder, M. E. (2004) Palmitoylation of intracellular signaling proteins: regulation and function. *Annu. Rev. Biochem.* **73**, 559–587
17. Valdez-Taubas, J., and Pelham, H. R. (2003) Slow diffusion of proteins in the yeast plasma membrane allows polarity to be maintained by endocytic cycling. *Curr. Biol.* **13**, 1636–1640
18. Warren, D. T., Andrews, P. D., Gourlay, C. W., and Ayscough, K. R. (2002) Sla1p couples the yeast endocytic machinery to proteins regulating actin dynamics. *J. Cell Sci.* **115**, 1703–1715
19. Siniossoglou, S., Peak-Chew, S. Y., and Pelham, H. R. (2000) Ric1p and Rgp1p form a complex that catalyses nucleotide exchange on Ypt6p. *EMBO J.* **19**, 4885–4894
20. Martin, B. R., and Cravatt, B. F. (2009) Large-scale profiling of protein palmitoylation in mammalian cells. *Nat. Methods* **6**, 135–138
21. Hang, H. C., Geutjes, E. J., Grotenbreg, G., Pollington, A. M., Bijlmakers, M. J., and Ploegh, H. L. (2007) Chemical probes for the rapid detection of Fatty-acylated proteins in Mammalian cells. *J. Am. Chem. Soc.* **129**, 2744–2745
22. Wang, Y. X., Catlett, N. L., and Weisman, L. S. (1998) Vac8p, a vacuolar protein with armadillo repeats, functions in both vacuole inheritance and protein targeting from the cytoplasm to vacuole. *J. Cell Biol.* **140**, 1063–1074
23. Veit, M., Kretzschmar, E., Kuroda, K., Garten, W., Schmidt, M. F., Klenk, H. D., *et al.* (1991) Site-specific mutagenesis identifies three cysteine residues in the cytoplasmic tail as acylation sites of influenza virus hemagglutinin. *J. Virol.* **65**, 2491–2500
24. Charollais, J., and Van Der Goot, F. G. (2009) Palmitoylation of membrane proteins (Review). *Mol. Membr. Biol.* **26**, 55–66
25. Valdez-Taubas, J., and Pelham, H. (2005) Swf1-dependent palmitoylation of the SNARE Tlg1 prevents its ubiquitination and degradation. *EMBO J.* **24**, 2524–2532
26. Tarassov, K., Messier, V., Landry, C. R., Radinovic, S., Serna Molina, M. M., Shames, I., *et al.* (2008) An in vivo map of the yeast protein interactome. *Science* **320**, 1465–1470
27. Weill, U., Cohen, N., Fadel, A., Ben-Dor, S., and Schuldiner, M. (2019) Protein topology prediction algorithms Systematically investigated in the yeast Saccharomyces cerevisiae. *Bioessays* **41**, e1800252
28. Babu, P., Deschenes, R. J., and Robinson, L. C. (2004) Akr1p-dependent palmitoylation of Yck2p yeast casein kinase 1 is necessary and sufficient for plasma membrane targeting. *J. Biol. Chem.* **279**, 27138–27147
29. Papanayotou, I., Sun, B., Roth, A. F., and Davis, N. G. (2010) Protein aggregation induced during glass bead lysis of yeast. *Yeast* **27**, 801–816
30. Roth, A. F., Feng, Y., Chen, L., and Davis, N. G. (2002) The yeast DHHC cysteine-rich domain protein Akr1p is a palmitoyl transferase. *J. Cell Biol.* **159**, 23–28
31. Schuldiner, M., Metz, J., Schmid, V., Denic, V., Rakwalska, M., Schmitt, H. D., *et al.* (2008) The GET complex mediates insertion of tail-anchored proteins into the ER membrane. *Cell* **134**, 634–645
32. Guna, A., Volkmar, N., Christianson, J. C., and Hegde, R. S. (2018) The ER membrane protein complex is a transmembrane domain insertase. *Science* **359**, 470–473
33. Chitwood, P. J., Juszkiewicz, S., Guna, A., Shao, S., and Hegde, R. S. (2018) EMC is required to Initiate accurate membrane protein topogenesis. *Cell* **175**, 1507–1519.e1516
34. Abrami, L., Leppla, S. H., and van der Goot, F. G. (2006) Receptor palmitoylation and ubiquitination regulate anthrax toxin endocytosis. *J. Cell Biol.* **172**, 309–320
35. Gao, Z., Ni, Y., Szabo, G., and Linden, J. (1999) Palmitoylation of the recombinant human A1 adenosine receptor: enhanced proteolysis of palmitoylation-deficient mutant receptors. *Biochem. J.* **342**, 387–395
36. Percherancier, Y., Planchenault, T., Valenzuela-Fernandez, A., Virelizier, J.-L., Arenzana-Seisdedos, F., and Bachelerie, F. (2001) Palmitoylation-dependent control of degradation, life span, and membrane expression of the CCR5 receptor. *J. Biol. Chem.* **276**, 31936–31944
37. Mukhopadhyay, K., Kohli, A., and Prasad, R. (2002) Drug susceptibilities of yeast cells are affected by membrane lipid composition. *Antimicrob. Agents Chemother.* **46**, 3695–3705
38. Belgareh-Touze, N., Leon, S., Erpapazoglou, Z., Stawiecka-Mirota, M., Urban-Grimal, D., and Haguenauer-Tsapis, R. (2008) Versatile role of the yeast ubiquitin ligase Rsp5p in intracellular trafficking. *Biochem. Soc. Trans.* **36**, 791–796
39. Dunn, R., and Hicke, L. (2001) Multiple roles for Rsp5p-dependent ubiquitination at the internalization step of endocytosis. *J. Biol. Chem.* **276**, 25974–25981
40. Gupta, R., Kus, B., Fladd, C., Wasmuth, J., Tonikian, R., Sidhu, S., *et al.* (2007) Ubiquitination screen using protein microarrays for comprehensive identification of Rsp5 substrates in yeast. *Mol. Syst. Biol.* **3**, 116
41. Sudol, M. (1996) Structure and function of the WW domain. *Prog. Biophys. Mol. Biol.* **65**, 113–132
42. Sullivan, J. A., Lewis, M. J., Nikko, E., and Pelham, H. R. (2007) Multiple interactions drive adaptor-mediated recruitment of the ubiquitin ligase rsp5 to membrane proteins *in vivo* and *in vitro*. *Mol. Biol. Cell* **18**, 2429–2440
43. Nikko, E., Sullivan, J. A., and Pelham, H. R. (2008) Arrestin-like proteins mediate ubiquitination and endocytosis of the yeast metal transporter Smf1. *EMBO Rep.* **9**, 1216–1221
44. Rana, M. S., Kumar, P., Lee, C. J., Verardi, R., Rajashankar, K. R., and Banerjee, A. (2018) Fatty acyl recognition and transfer by an integral membrane S-acyltransferase. *Science* **359**, eaao6326
45. Gonzalo, S., and Linder, M. E. (1998) SNAP-25 palmitoylation and plasma membrane targeting require a functional secretory pathway. *Mol. Biol. Cell* **9**, 585–597
46. Ponimaskin, E., and Schmidt, M. F. (1995) Acylation of viral glycoproteins: structural requirements for palmitoylation of transmembrane proteins. *Biochem. Soc. Trans.* **23**, 565–568
47. Bijlmakers, M. J., and Marsh, M. (2003) The on-off story of protein palmitoylation. *Trends Cell Biol.* **13**, 32–42
48. Robinson, L. C., Bradley, C., Bryan, J. D., Jerome, A., Kweon, Y., and Panek, H. R. (1999) The Yck2 yeast casein kinase 1 isoform shows cell cycle-specific localization to sites of polarized growth and is required for proper septin organization. *Mol. Biol. Cell* **10**, 1077–1092
49. Snowdon, C., and Johnston, M. (2016) A novel role for yeast casein kinases in glucose sensing and signaling. *Mol. Biol. Cell* **27**, 3369–3375
50. Kihara, A., Kurotsu, F., Sano, T., Iwaki, S., and Igarashi, Y. (2005) Long-chain base kinase Lcb4 Is anchored to the membrane through its palmitoylation by Akr1. *Mol. Cell. Biol.* **25**, 9189–9197
51. Birchwood, C. J., Saba, J. D., Dickson, R. C., and Cunningham, K. W. (2001) Calcium influx and signaling in yeast stimulated by intracellular sphingosine 1-phosphate accumulation. *J. Biol. Chem.* **276**, 11712–11718
52. Jenkins, G. M., Richards, A., Wahl, T., Mao, C., Obeid, L., and Hannun, Y. (1997) Involvement of yeast sphingolipids in the heat stress response of Saccharomyces cerevisiae. *J. Biol. Chem.* **272**, 32566–32572
53. Coronel Arrechea, C., Giolito, M. L., Garcia, I. A., Soria, G., and Valdez Taubas, J. (2021) A novel yeast-based high-throughput method for the identification of protein palmitoylation inhibitors. *Open Biol.* **11**, 200415
54. Quiroga, R., Trenchi, A., Gonzalez Montoro, A., Valdez Taubas, J., and Maccioni, H. J. (2013) Short transmembrane domains with high-volume exoplasmic halves determine retention of Type II membrane proteins in the Golgi complex. *J. Cell Sci.* **126**, 5344–5349

55. Sievers, F., Wilm, A., Dineen, D., Gibson, T. J., Karplus, K., Li, W., *et al.* (2011) Fast, scalable generation of high-quality protein multiple sequence alignments using Clustal Omega. *Mol. Syst. Biol.* **7**, 539
56. Waterhouse, A. M., Procter, J. B., Martin, D. M., Clamp, M., and Barton, G. J. (2009) Jalview Version 2–a multiple sequence alignment editor and analysis workbench. *Bioinformatics* **25**, 1189–1191
57. McGuffin, L. J., Bryson, K., and Jones, D. T. (2000) The PSIPRED protein structure prediction server. *Bioinformatics* **16**, 404–405
58. Schindelin, J., Arganda-Carreras, I., Frise, E., Kaynig, V., Longair, M., Pietzsch, T., *et al.* (2012) Fiji: an open-source platform for biological-image analysis. *Nat. Methods* **9**, 676–682